Solid electrolyte interphases at Li-ion battery graphitic anodes in propylene carbonate (PC)-based electrolytes containing FEC, LiBOB, and LiDFOB as additives

Mahesh Datt Bhatt

Department of Chemistry, University College Cork, Cork, Ireland

Colm O'Dwyer*

Department of Chemistry, University College Cork, Cork, Ireland

Micro and Nanoelectronics Centre, Tyndall

National Institute, Lee Maltings, Cork, Ireland and

Email: c.odwyer@ucc.ie; Tel: +353 (0)21 4902732; Fax: +353 (0)21 4274097

Abstract

Density functional theory is used to investigate the reactivity, reduction and effect of electrolyte additives such as fluoroethylene carbonate (FEC), lithium bis(oxalate) borate (LiBOB) and lithium difluoro(oxalato) borate (LiDFOB) in propylene carbonate (PC)-based Li-ion battery electrolytes. The structural, thermodynamical and calculated infra-red vibrational analyses indicate that the FEC additives reduction prior to PC, providing stable SEI film formation near the graphite anode. The reduction and reaction mechanisms of LiBOB and LiDFOB influence the SEI film composition at the graphite surface. These additives contribute to stable SEI film formation without degradation of the anode structure by PC co-intercalation.

Keywords: Li-ion battery; electrolyte; additive; desnity functional theory; anode; SEI

INTRODUCTION

Lithium-ion batteries are very promising energy storage devices due to their high volumetric and gravimetric energy density [1, 2]. While current Li-ion battery technology is adequate for certain portable electronic applications, the increased power demand of electric vehicles and high power demand consumer electronics require development of anode and cathode materials, and electrolyte systems capable of supporting high energy density in a stable manner. Much of the processes and mechanisms underpinning carbonate-based electrolytes in Li-ion batteries, particularly at the anode, still need to be resolved [3]. Solid electrolyte interphase (SEI) films that form on the surfaces of low voltage anodes during electrolyte decomposition reactions provide electrode surface stability, affecting electron transfer reactions and allowing Li^+ transport during reversible charging and discharging [4, 5] reactions. The structure and composition in common electrolytes has recently been established using a variety of experimental probes [6, 7].

Some commonly used organic solvents include ethylene carbonate (EC), propylene carbonate (PC), dimethyl carbonate (DMC), diethyl carbonate (DEC), ethyl methyl carbonate (EMC) etc. These organic electrolytes are decomposed during intercalation of lithium ions into graphitic anodes resulting in the formation of the crucial solid electrolyte interphase (SEI) film [8–10]. The decomposition mechanism of an organic solvent and subsequent formation of SEI films near the graphite anode is an important research topic in lithium ion batteries from theoretical [11–15] and experimental [16–25] standpoints. In electrolytes that contain stable SEI-promoting additives, and for salts that promote SEI formation, many fundamental questions concerning the mechanisms of electrolyte decomposition and SEI structure formation remain open. Processes from ionic liquid electrolytes in the vicinity of complex, higher surface energy nanomaterial anodes also require investigation. Using models based on electronic structure, the understanding of specific reaction pathways, some of which are difficult to isolate in experiment, can be interrogated.

It is well known that PC is less suitable as an electrolyte for graphitic anodes compared to EC and others due co-intercalation of solvent molecules into graphite during the first charge process [26]. This effect can lead to the destruction of the graphite structure via several mechanisms including gas evolution, competitive interactions overcoming van der Walls forces in graphitic anodes, swelling and chemical and machanical exfoliation [27–29]. There-

fore, many methods have been developed to solve this problem. One effective method is the use of film-forming electrolyte additives which are reduced predominantly on the graphite anode surface during the first charging process. The reason is that the additives are able to: (i) facilitate stable SEI formation on the surface of graphite, (ii) reduce irreversible capacity and gas generation that in some cases can accompany SEI formation to improve stability in long-term cycling, (iii) enhance thermal stability of $LiPF_6$ and related lithium salts against organic electrolyte solvents, (iv) protect the cathode material from dissolution and overcharge, and (v) improve physical properties of the electrolyte such as ionic conductivity, viscosity, and wettability to the separator. For safer Li-ion batteries, electrolyte additives offer: (i) better flammability limits of organic electrolytes, (ii) a decrease in overcharge potential, and (iii) termination of battery operation under abusive operating conditions. The effect of added fluoroethylene carbonate (FEC) to $LiPF_6$ electrolytes on the cycling performance of silicon anodes has been investigated [30, 31] to understand decomposition mechanisms that lead to Li^+ conductive SEI films. Other salt-based additives, namely lithium bis(oxalate) borate (LiBOB, see Fig. 2) and lithium difluoro-(oxalato) borate (LiDFOB), have attracted interest due to their ability to promote stable SEI formation.

Although LiBOB was first proposed as a replacement for $LiPF_6$ salt in electrolytes [32, 33], at low conentrations ($\approx$1 wt %) it can be considered an electrolyte additive [34]. Benefits include improved anodic stability when Al current collectors are used [35], stabilization of electrolyte at high temperature and potentials [36], and more durable and stable SEI on graphitic anodes [37–39] during cycling. Like LiBOB, LiDFOB at additive-level concentrations has the innate ability to form a SEI on the surface of a graphite anode, even in high concentrations of PC [40]. With the advent of many new forms of anode materials, with a wide range of active nanostructured forms, the understanding of electrolyte, salt and additive mixtures on the formation of SEI layers is important. This intrinsic property of a lithium salt dominating SEI formation is necessary for the replacement of the high-melting EC that is typically required for SEI formation. LiDFOB also possesses characteristics similar to $LiBF_4$ such as an exceptional ability to passivate the Al current collector [41]. Although FEC, LiBOB and LiDFOB are promising additives for PC-based electrolytes in Li-ion graphitic anodes, no DFT calculations have been reported thus far that investigate the supportive role of these additives in PC-based electrolytes regarding SEI film formation near graphitic anodes in Li-ion batteries.

In this work, we first investigate the electronic structure of Li^+-PC and Li^+-PC-C_6 without additives and then with important additives such as fluoroethylene carbonate (FEC), lithium bis(oxalate) borate (LiBOB) and lithium difluoro(oxalato) borate (LiDFOB). From computations we compare their relative effectiveness and influence on the structure of PC and lithiated PC eletrolytes and its ability to promote a stable SEI film structure near a graphite anode.

COMPUTATIONAL DETAILS

An isolated PC solvent and electrolyte additive (FEC, LiBOB, LiDFOB) molecule and their clusters including a Li^+ ion and graphite (C_6) are optimized by using the B3LYP/6-31G (d) parameter in the gas phase. FEC, LiBOB, and LiDFOB are all referred to as additives in this work. Density functional theory calculations are performed with hybrid parameter B3LYP as implemented in Gaussian 09W. The hybrid parameter B3LYP consists of exchange correlation function generalized gradient approximation (GGA) in the Becke [42], Lee-Yang-Parr [43], and VWN formula 5 [44]. The basis set is chosen as 6-31G (d) for our calculations. The approximate basis set superposition error (BSSE) [45] for all clusters is calculated using Counter Poise (CP) method and is observed to be negligibly small. The first electron reduction energy ($E_1 = E_{11} + E_{12}$) and the second electron reduction energy (E_2) for PC and additives are calculated according to the reduction schemes as illustrated in Ref. [12]. The calculated optimized structures of propylene carbonate (PC), fluoroethylene carbonate (FEC), lithium bis(oxalate) borate (LiBOB), lithium difluoro(oxalato) borate (LiDFOB), and graphite intercalation compound (C_6) are shown in Supplementary Materials, Fig. S1. The optimized structures of the lithiated cluster Li^+(PC) and Li^+(PC)(A) [A = FEC, LiBOB, LiDFOB] complexes are shown in Fig. 1.

RESULTS AND DISCUSSION

Energetics and structure of PC electrolytes with FEC, LiBOB and LiDFOB

The energetics of PC and additives (A = FEC, LiBOB and LiDFOB) as well as their first and second electron reduction energies are determined. The frontier molecular orbital

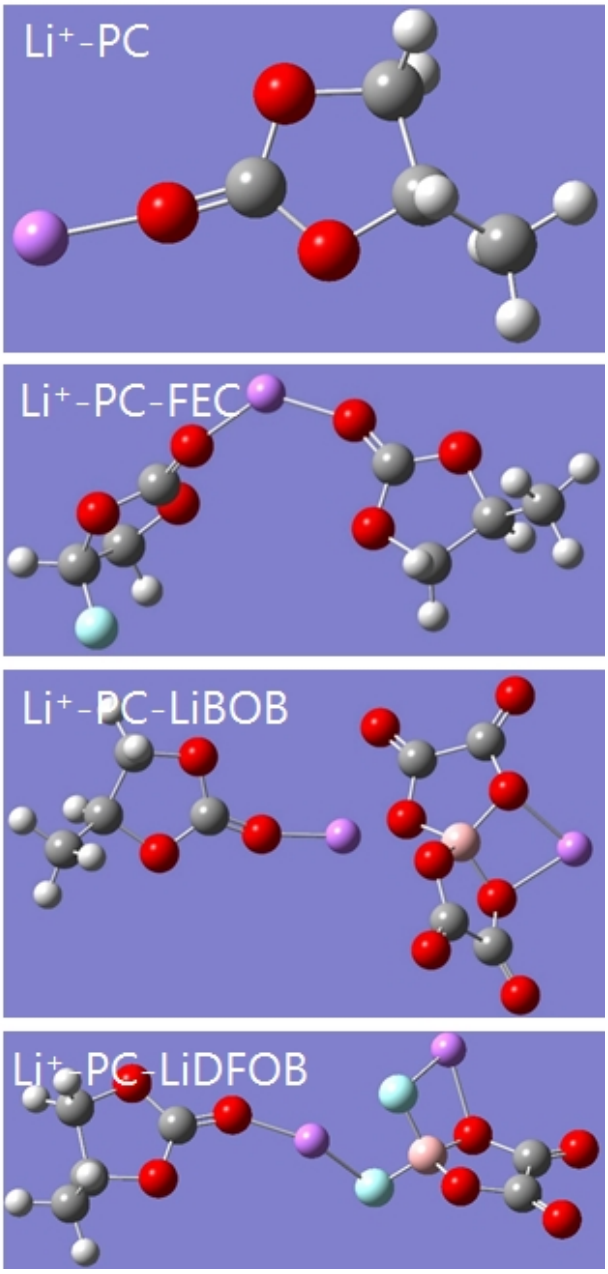

FIG. 1. Optimized structures of Li^+-PC and Li^+-PC-A [A = FEC, LiBOB, and LiDFOB] complexes.

energy of additives (A = FEC, LiBOB and LiDFOB) and PC are shown in Supplementary Materials, Table S1.

From Table S1, we observe that the energy level of the LUMO of any additive A is much lower than that of PC solvent itself. Based upon molecular orbital theory, a molecule with lower LUMO energy should be a better acceptor and more reactive on the negatively charged

surface of the anode. FEC, LiBOB and LiDFOB will be reduced prior to the PC solvent during the first charge process. The reactivity of additives based on the LUMO energy and HOMO-LUMO gap follows the order LiDOB > LiDFOB > FEC. The dipole moment also indicates that LiBOB and LiDFOB are more stable than FEC.

Table S2, Supplementary Materials, lists the calculated first and second electron reduction energies of PC and all additives. FEC exhibits a first electron reduction energies (E_1) energetically more favourable than PC. If the charging process is electrochemically limited to the first electron reduction for PC-based electrolyte, the FEC additive (-3.27 eV) is most effective in promoting SEI film formation. The second electron reduction energy (E_2) follows a similar trend. Here, FEC is capable of undergoing a second electron reduction to produce Li_2CO_3 and other components of the SEI film via interactions with the PC electrolyte. A detailed investigation of 1- and 2-electron mechanisms of FEC reduction in EC has been reported elsewhere [49]. Although LiBOB and LiDFOB have been demonstrated to be promising salts/additives in PC-based electrolytes, the first and second electron reduction energies are not consistent with those for FEC by a similar mechanism. LiBOB and LiDFOB are considered as reaction-type additives and FEC is reductive-type additive [41]. Previous experimental results have demonstrated that LiBOB electrolytes involve the reduction of the BOB anion at relatively high potentials (> 1 V) to form the SEI layer and prevent PC co-intercalation, but the mechanism is still unclear. Our calculations shows that reduction mechanisms are feasible, but less favourable than PC, particularly for the first electron reduction process in the gas phase (which has a limited Li^+ co-ordination sphere). In Fig. 2, the optimized structure of the anions confirms a linearization of the FEC after reduction, but aside from ring opening, the reduced structures of LiBOB and LiDFOB are not linear thus confirming the simpler reduction mechanism compared to carbonate additives. PC alone may be decomposed before undergoing second electron reduction due to higher value of E_2.

Calculated IR spectra of reductively and reactively formed SEI phases from PC-additive electrolytes

LiBOB and LiDFOB are believed to stabilize SEI formed in PC-based electrolytes due to presence of B-O moieties in the resulting SEI film. Experimental evidence from FTIR and

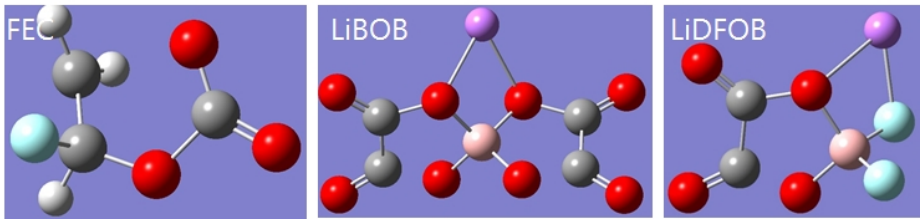

FIG. 2. Optimized anions after first electron reduction of FEC, LiBOB and LiDFOB.

XPS measurements from cycled graphite electrodes in such electrolytes confirmed [39, 41, 46, 47] their presence within the SEI composition.

Experimental FTIR results [39] obtained by substraction of the pure IR spectrum of PC from that of PC/LiBOB indicated that the electrochemical reduction of the LiBOB and LiDFOB anions forms part of the SEI layer chemistry. For example, in a PC-LiBOB electrolyte, the BOB anion is solvated by the PC molecule and ion-pairing interactions may complicate Li^+ co-ordination. To directly determine the structure of the solvated BOB anion, we performed DFT calculations to calculate the vibrational properties and compare the spectrum to that obtained by subtraction of the PC/LiBOB and PC data from experiment. The calculated vibrational frequencies of the solvated BOB anion are shown in Fig. 4(b) (with the relevant calculated IR spectrum for free BOB anion shown in Fig. 3 (a)) and band assignments are summarized in Supplementary Materials, Table S3. There is good agreement between calculated and experimental frequencies of BOB anion, confirming the assignments are consistent with the experimental IR spectra.

Separately, we calculated the IR spectra for solvated BOB in PC, in addition to that of PC and PC-LiBOB from optimized structures (Fig. 3) to compare to experimental spectra [38, 39] obtained after charge-discharge cycling. A switch in the intensity of the two C=O stretches (sym. and asym.) are found in PC-solvated BOB anions compared to free BOB. B-O-C and O-B-O asymmetric vibrations characteristic of free BOB are significantly constrained in the solvated BOB anion. The IR spectra of BOB anion in PC along with isolated PC and LiBOB in PC are shown in Fig. 3(b). These IR spectra are consistent with FTIR spectra where the solvated BOB in PC spectrum was not obtained directly.

The nature of the SEI layer structure formed in PC-LiBOB electrolytes is still unclear in some aspects, as is the case for LiDFOB-based systems. Previous analyses suggested that unreacted BOB anions are part of the SEI layer in PC-LiBOB electrolytes, implying

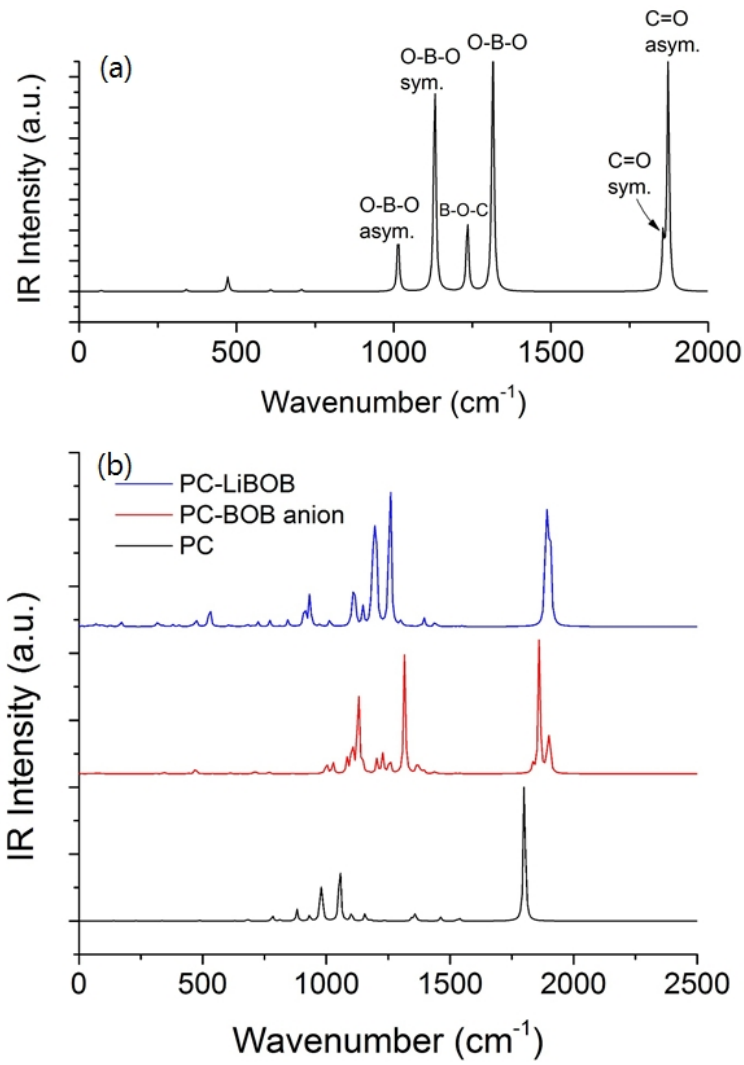

FIG. 3. Calculated IR spectrum of (a) free BOB anion as an example, and (b) of BOB anion in PC together with isolated PC and LiBOB in PC.

a series of more complicated exchange reactions between B-O and R-O (R = alkyl moiety) bonds forming the charge products, as opposed to species formed by electron transfer. This situation is specifically different to SEI formed in standard EC-DMC based electrolytes containing $LiPF_6$ at a carbon surface. A comparison of the DFT calculated spectra of the surface layers formed after the anode is cycled in PC-LiBOB compared to EC-EMC-$LiPF_6$ is shown in Fig. 4 along with the optimized structure of EC-EMC-$LiPF_6$ complex. These structures are determined without the complication of interactions with a graphite surface, which can be difficult to avoid in experiment. Experimentally, the C=O vibrations observed

in the BOB anion in PC are found after cycling in the PC-LiBOB system, and confirmed through calculations. However, strong sym. and asym. C=O stretches are also present in the pure PC but at a slightly lower energy since they are comparatively unconstrained in the resulting structure. With the graphite surface excluded, the resulting vibrational signature of the PC-LiBOB compared to EC-EMC-$LiPF_6$ is markedly different to experimental spectra acquired of the resulting SEI layer on the carbon surface. The DFT spectra avoid the carbon surface influence on bonding and any possiblity of dried salt contributions, in order to deduce the interaction. Figure 4(a) confirms that no vibrational features are evident in the range 1400-1650 cm^{-1} in the IR spectra from PC-LiBOB nor EC-EMC-$LiPF_6$ complex, although they have been reported from experimentally cycled carbon anodes. Little evidence for carboxylates or lithium carbonate found in EC-EMC-$LiPF_6$ is found in calculations of structures in the gas phase. Based on subtraction of the spectra in Fig. 5(a), substrate-independent vibational features in PC-LiBOB from species close to orthoborates are found in the range 1100-1370 cm^{-1}. Detailed FTIR studies of carbon anodes in these electrolytes citing vibrational contributions from borates, oxalates and methoxides etc. that contribute to experimentally observed spectra are reported elsewhere [39].

With calculations for the optimized lithiated solvent complexes, the energetics of ternary graphite intercalation compounds (GICs) without additive as Li^+-PC-C_6 and with additives as Li^+-PC-A-C_6 (A = FEC, LiBOB and LiDFOB) can be examined as a model system replicating a graphite anode PC electrolytes with and without these additives. The optimized structures of Li^+-PC and Li^+-PC-A complexes (A = FEC, LiBOB and LiDFOB) are shown in Fig. 5. The ternary GIC energy is calculated according to:

$$\Delta E[Li^+ - PC - C_6 - A] = E_{total}[Li^+ - PC - C_6] + E_{total}[Li^+ - PC] - E[C_6] - E[A]$$

where $E_{total}[Li^+ - PC - C_6]$, $E_{total}[Li^+ - PC]$, $E[C_6]$, and $E[A]$ represent the total free energy of a GIC, a solvent PC molecule, graphite, and additive molecule respectively. The GIC intercalation energies of Li^+-PC and Li^+-PC-A complexes (A = FEC, LiBOB and LiDFOB) are provided in Supplementary Materials, Table S4. From Table S4, the intercalation energy of Li^+-PC-C_6 complex increases by a factor of ≈2-3× with all additives FEC, LiBOB and LiDFOB, indicating their thermodynamic stability in PC-based electrolytes at graphite anodes for SEI formation.

Calculations defining the characteristics and structure of Li^+-PC, and each case with

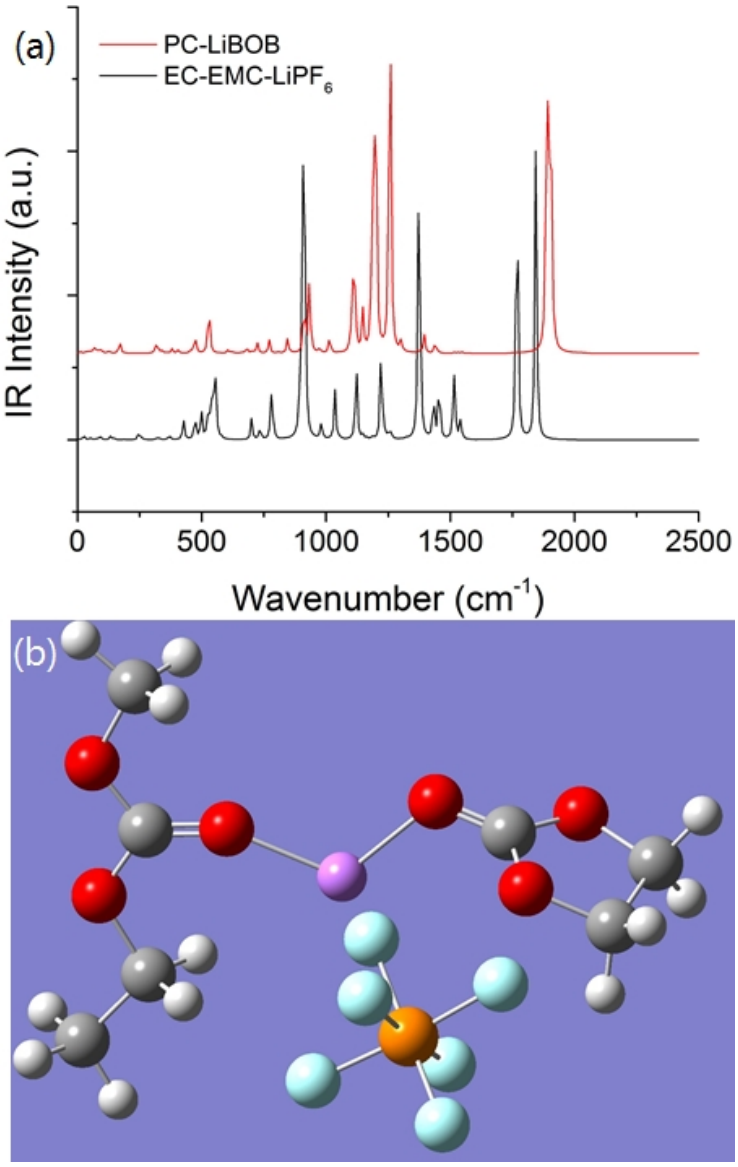

FIG. 4. IR spectra of PC-LiBOB vs. EC-EMC-$LiPF_6$ and (b) optimized structure of EC-EMC-$LiPF_6$.

additives (A= FEC, LiBOB and LiDFOB) considered as model complexes, are summarized in Table S5, Supplementary Materials.

From Table S5, the change in Gibbs free energy and enthalpy scale as FEC > LiBOB > LiDFOB, which is inconsistent with the observed order of their respective LUMO energies and HOMO-LUMO gaps. This differences is ascribed to the strong effect of the graphite intercalation compound (C_6) on FEC as reductive additive and relatively lower, but measureable effect on both reactive additives LiBOB and LiDFOB. The minimum C=O bond

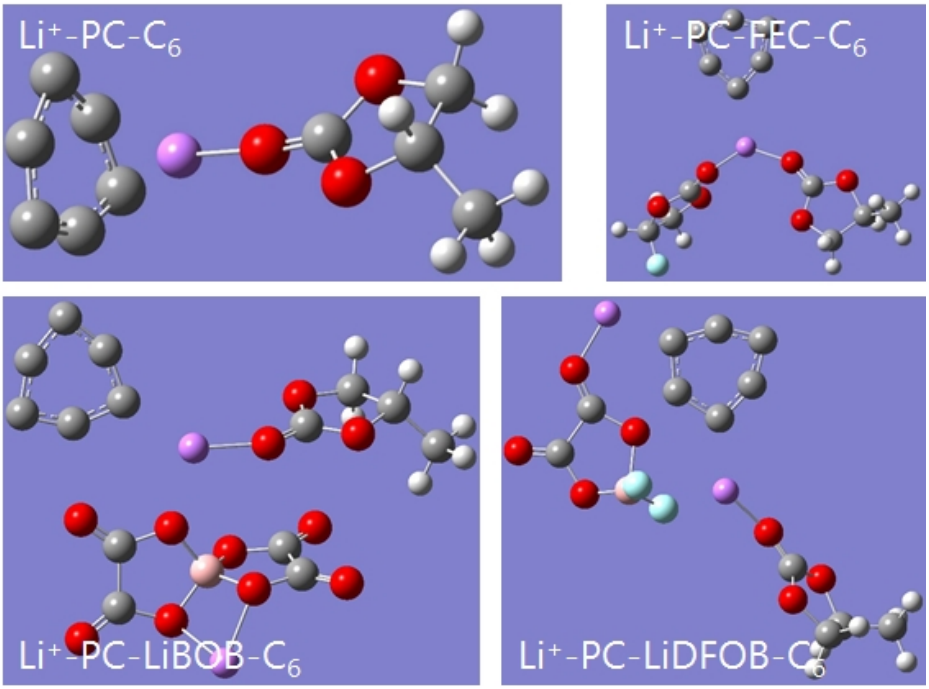

FIG. 5. Optimized structures of Li^+-PC-C_6 and Li^+-PC-A-C_6 complexes (A = FEC, LiBOB, and LiDFOB).

length calculated for Li^+-PC-C_6 decreases by a maximum of 0.009 Å, while C-O bong length increases by 0.005-0.006 Å when additives are used. The minimum Li^+-O distance in Li^+-PC-C_6 is found to increase by a maximum of 0.097 Å when FEC is used, 0.082 Å for LiBOB, and 0.067 Å for LiDFOB. The magnitude of spectral shifts here can often be a function of the basis set and the exchange-correlation functional to some extent, adding complexity to direct experimental comparison under liquid (electrochemical) conditions, hence the comparative calculations with and without substrate interactions.

The theoretical IR spectra of Li^+-PC-C_6 with and without additives (A= FEC, LiBOB and LiDFOB) are calculated and analyzed comparatively. The IR spectra of Li^+-PC and Li^+-PC-A complexes are shown in Figs 6 (a) and (b) respectively. By comparison the the spectra in Fig. 4 calculated without the influence of the graphite substrate, specific differences are found. In Fig. 6(a), the vibrational signature of Li^+-PC-C_6 shows additional C=O stretches due to the influence of the graphite substrate. From Fig. 6(b), we note that the C=O and C-O frequencies of PC change in the same order as the change in their respective bond lengths due to interactions from additives, as shown in Table S5. The C=O regions are

considerably more complex due to interactions of the solvated Li^+ in PC with additives (*cf.* Fig. 3(b)). During a process that is designed to mimic electrochemical reduction of species during charging, the LiBOB and LiDFOB salts at additive level to PC electrolytes do not reduce via classic two-step electron reduction mechanisms but via reaction pathways. The energetics from calculation prove their applicability in preventing PC co-intercalation by preferentially allow reactions (or complete reduction in the case of FEC additives) prior to that of PC. The calculated IR spectra with and without additives, and alone or in the vicinity of a carbon surface, indicate that the oxygen bond with boron is not broken in this case to form orthoborates [33], and the C=O frequencies cannot be explicitly identified as coming from O-C-O functional groups in oxalates from the Li salt. Similar vibrations are found in the case of LiDFOB, although somewhat convoluted with C=O groups. Specific vibrational contributions from polycarbonate species in PC and PC/FEC containing electrolytes are not clearly observed when the C_6 is considered, although in a high dielectric environment such as the electrolyte (not factored identically in the gas phase calculations in this work), their presence is prone to further electrochemcial reduction as observed in FEC-additive containing electrolytes and silicon anodes [48].

Recently, the SEI layers formed in electrolytes containing FEC at silicon surfaces (in EC however) were examined using DFT [49]. These investigations disputed previously reported reaction pathways involving HF and CH_2CHF during FEC decomposition at lower voltages. While the case of silicon is unique, owing to the possibility for strong H- and F-bonding to its surface, those calculations posited that HF and CH_2CHF are not released during its decomposition. LiF is proposed as a primary product of these SEI films, which may also occur from $LiPF_6$ in cases where H_2O is present [6, 50]. Our calculations of low quantities of FEC in PC at a graphite surface confirm reduction of the FEC in order to provide Li^+ conducting species in the SEI without co-intercalation of the PC molecule. The 2-electron FEC reduction avoids a charge-neutral product that hampers Li^+ conductivity, thereby limiting an effective and stable SEI film at the graphite surface.

Examination of IR spectra in the C-H region (Fig. 7) confirms that sym. and asym. C-H stretches around 3000 cm^{-1} are found for the F-containing Li^+-PC-A-C_6 complexes (A = FEC and LiDFOB) systems. Very low intensity C-H vibrations are found for Li^+-PC-LiBOB-C_6 phase, but can be discerned. The primary difference in the IR response are interactions due to the graphite, not found in pure PC. In F-containing additives (FEC) and salts

(LiDFOB) analysis was compared to CH_2CHF vibrations on the basis of eigenvectors of the normal vibrational modes using symmetry classification of an interacting CH_2CHF molecule. While LiF is a likely component of SEI using FEC for either a 1- or 2-electron reduction, the theoretical IR spectra were scanned for C-F stretch and C=C-F planar deformation vibrations for Li^+-PC-A complexes (A = FEC, LiBOB and LiDFOB), with and without the graphite surface. C-F stretches are found at 1027 and 1064 cm^{-1} for Li^+-PC-FEC-C_6 and Li^+-PC-LiDFOB-C_6, but not in LiBOB complexes nor any non-F-containing systems in this study; no clear evidence for C=C-F is observed. A peak at 1035 cm^{-1} is found for the EC/EMC/$LiPF_6$ system, but calculations (see Fig. 3) are independent of interactions with graphite. We emphasize that in the case of LiDFOB, the final structure is not entirely reduced, but likely a participant in the final reaction product associated with the SEI layer.

CONCLUSIONS

Density functional theory methods were used to investigate the effect of electrolyte additives such as fluoroethylene carbonate (FEC), lithium bis(oxalate) borate (LiBOB) and lithium difluoro(oxalato) borate (LiDFOB) in propylene carbonate (PC)-based Li-ion battery electrolytes in the gas phase at the level of B3LYP/6-31G (d). The reactivity of the additives under consideration follows LiBOB > LiDFOB > FEC based on their respective LUMO energy levels and HOMO-LUMO gap energies. Calculations demonstrate that the reduction decomposition of PC and electrolyte additives is such that the first electron reduction in the gas phase is found in the order FEC > PC. The reactive additives LiBOB and LiDFOB do not follow the two step electron reduction mechanism for PC-based electrolytes during SEI formation near the graphite anode, resulting in specific species formed in the SEI layer. Theoretical IR vibrational characteristics of PC with and without additives also indicate the bonding within solvated complexes, indicating that at low concentrations and considered as an eletrolyte additive salt, a stable SEI film formation takes place in the presence of a graphitic surface. Calculation with and without the graphite surface interactions allowed examination of PC and additive decomposition and structure. Subsequent PC reduction occurs on a surface with preformed species from the additives and salts, thereby helping to prevent PC co-intercalation. The data demonstrate the supportive role of certain additives namely LiBOB and LiDFOB in PC-based electrolytes for SEI film formation and

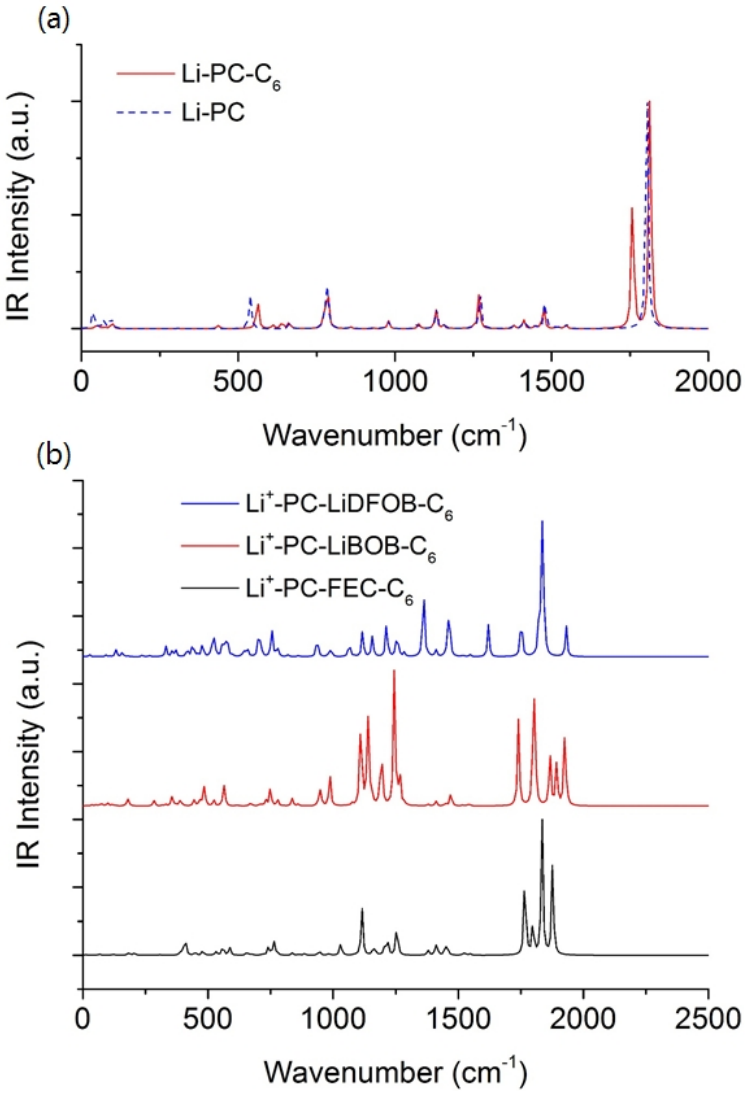

FIG. 6. IR spectra of (a) Li^+-PC-C_6 and (b) Li^+-PC-C_6-A complexes (A= FEC, LiBOB and LiDFOB).

stable cycling at graphitic carbon-based Li-ion battery anodes without degradation of the anode structure.

ACKNOWLEDGEMENTS

We acknowledge Science Foundation Ireland (SFI) and the Higher Education Authority for computing time at the Irish Centre for High-End Computing (ICHEC). This research has received funding from the Seventh Framework Programme FP7/2007-2013 (Project STA-

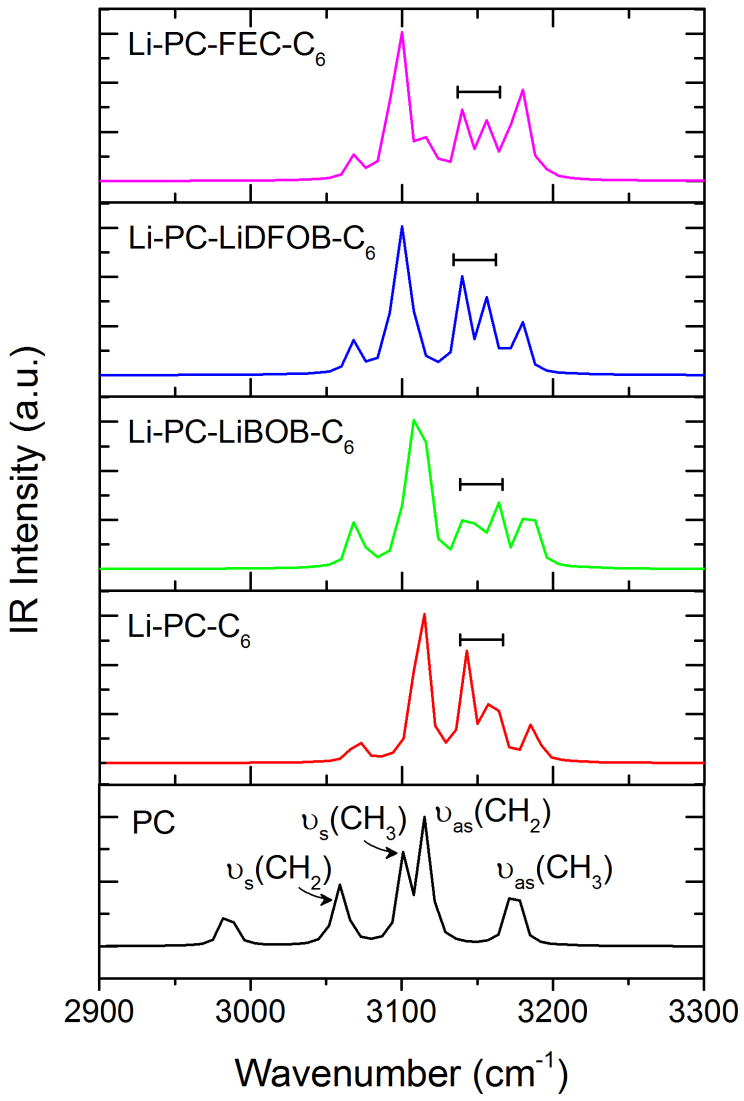

FIG. 7. C-H sym. and asym. vibrations for PC, Li^+-PC-C_6, and Li^+-PC-C_6-A.

BLE) under grant agreement No. 314508.

[1] Owen, J. R., *Chem. Soc. Rev.* **1997**, *26*, 259-267.

[2] Wang, Y.; Cao, G., *Adv. Mater.* **2008**, *20*, 2251-2269.

[3] Goodenough, J. B., *Acc. Chem. Res.* **2012**, *46*, 1053-1061.

[4] Leung, K., *Chem. Phys. Lett.* **2013**, *568-569*, 1-8.

[5] McSweeney, W.; Lotty, O.; Glynn, C.; Geaney, H.; Holmes, J. D.; O'Dwyer, C., *Electrochim. Acta* **2014**, *135*, 356-367.

[6] Nie, M., Chalasani, D., Abraham, D. P., Chen, Y., Bose, A. and Lucht, B. L., *J. Phys. Chem. C* **2013**, *117*, 1257-1267.

[7] Cresce, A. v.; Russell, S. M.; Baker, D. R.; Gaskell, K. J.; Xu, K., *Nano Lett.* **2014**, *14*, 1405-1412.

[8] Armand, M.; Tarascon, J.-M., *Nature* **2008**, *451*, 652-657.

[9] Osiak, M.; Geaney, H.; Armstrong, E.; O'Dwyer, C., *J. Mater. Chem. A* **2014**, *2*, 9433-9460.

[10] Armstrong, M. J.; O'Dwyer, C.; Macklin, W. J.; Holmes, J. D., *Nano Res.* **2014**, *7*, 1-62.

[11] Aurbach, D., *J. Power Sources* **2000**, *89*, 206-218.

[12] Aurbach, D.; Ein-Ely, Y.; Zaban, A., *J. Electrochem. Soc.* **1994**, *141*, L1-L3.

[13] Aurbach, D.; Markovsky, B.; Weissman, I.; Levi, E.; Ein-Eli, Y., *Electrochim. Acta* **1999**, *45*, 67-86.

[14] Xu, K.; von Cresce, A., *J. Mater. Chem.* **2011**, *21*, 9849-9864.

[15] Bhatt, M. D.; O'Dwyer, C., *J. Electrochem. Soc.* **2014**, *161*, A1415-A1421.

[16] Endo, E.; Ata, M.; Tanaka, K.; Sekai, K., *J. Electrochem. Soc.* **1998**, *145*, 3757-3764.

[17] Endo, E.; Tanaka, K.; Sekai, K., *J. Electrochem. Soc.* **2000**, *147*, 4029-4033.

[18] Han, Y.-K.; Lee, S. U.; Ok, J.-H.; Cho, J.-J.; Kim, H.-J., *Chem. Phys. Lett.* **2002**, *360*, 359-366.

[19] Li, T.; Balbuena, P. B., *Chem. Phys. Lett.* **2000**, *317*, 421-429.

[20] Marquez, A.; Balbuena, P. B., *J. Electrochem. Soc.* **2001**, *148*, A624-A635.

[21] Shu, Z.; McMillan, R.; Murray, J., *J. Electrochem. Soc.* **1993**, *140*, 922-927.

[22] Wang, Y.; Balbuena, P. B., *J. Phys. Chem. B* **2002**, *106*, 4486-4495.

[23] Wang, Y.; Balbuena, P. B., *J. Phys. Chem. A* **2002**, *106*, 9582-9594.

[24] Wang, Y.; Nakamura, S.; Tasaki, K.; Balbuena, P. B., *J. Am. Chem. Soc.* **2002**, *124*, 4408-4421.

[25] Kennedy, T.; Mullane, E.; Geaney, H.; Osiak, M.; O'Dwyer, C.; Ryan, K. M., *Nano Lett.* **2014** *14*, 716-723.

[26] Bhatt, M. D.; O'Dwyer, C., *Curr. Appl. Phys.* **2014**, *14*, 349-354.

[27] Fujimoto, M.; Shoji, Y.; Kida, Y.; Ohshita, R.; Nohma, T.; Nishio, K., *J. Power Sources* **1998**, *72*, 226-230.

[28] Kaneko, H.; Sekine, K.; Takamura, T., *J. Power Sources* **2005**, *146*, 142-145.

[29] Nicolosi, V.; Chhowalla, M.; Kanatzidis, M. G.; Strano, M. S.; Coleman, J. N., *Science* **2013**, *340* (6139).

[30] Choi, N.-S.; Yew, K. H.; Kim, H.; Kim, S.-S.; Choi, W.-U., *J. Power Sources* **2007**, *172*, 404-409.

[31] Nakai, H.; Kubota, T.; Kita, A.; Kawashima, A., *J. Electrochem. Soc.* **2011**, *158*, A798-A801.

[32] Lishka, U.; Wietelmann, U.; Wegner, M., Ger. Pet. DE 198290030 C1 (1999).

[33] Xu, W.; Shusterman, A. J.; Videa, M.; Velikov, V.; Marzke, R.; Angell, C. A., *J. Electrochem. Soc.* **2003**, *150*, E74-E80.

[34] Chen, Z.; Lu, W.; Liu, J.; Amine, K., *Electrochim. Acta* **2006**, *51*, 3322-3326.

[35] Zhang, X.; Devine, T. M., *J. Electrochem. Soc.* **2006**, *153*, B365-B369.

[36] Xiao, A.; Yang, L.; Lucht, B. L., *Electrochem. Solid-State Lett.* **2007**, *10*, A241-A244.

[37] Jiang, J.; Dahn, J., *Electrochem. Solid-State Lett.* 2003, 6 (9), A180-A182.

[38] Xu, K.; Lee, U.; Zhang, S.; Wood, M.; Jow, T. R., *Electrochem. Solid-State Lett.* **2003**, *6*, A144-A148.

[39] Zhuang, G.; Xu, K.; Jow, T.; Ross, P., *Electrochem. Solid-State Lett.* **2004**, *7*, A224-A227.

[40] Xu, K.; Zhang, S.; Poese, B. A.; Jow, T. R., *Electrochem. Solid-State Lett.* **2002**, *5*, A259-A262.

[41] Shui Zhang, S., *Electrochem. Commun.* **2006**, *8*, 1423-1428.

[42] Becke, A. D., *Phys. Rev. A* **1988**, *38*, 3098.

[43] Lee, C.; Yang, W.; Parr, R., *Phys. Rev. B* **1988**, *37*, 785-789.

[44] Vosko, S. H.; Wilk, L.; Nusair, M., *Can. J. Phys.* **1980**, *58*, 1200-1211.

[45] Boys, S. F.; Bernardi, F. D., *Mol. Phys.* **1970**, *19*, 553-566.

[46] Zhang, S.; Xu, K.; Jow, T., *J. Power Sources* **2004**, *129*, 275-279.

[47] Zhang, S.; Xu, K.; Jow, T., *J. Power Sources* **2006**, *156*, 629-633.

[48] Profatilova, I. A.; Stock, C.; Schmitz, A.; Passerini, S.; Winter, M., *J. Power Sources* **2013**, *222*, 140.

[49] Leung, K.; Rempe, S. B.; Foster, M. E.; Ma, Y.; Martinez del la Hoz, J. M.; Sai, N.; Balbuena, P. B., *J. Electrochem. Soc.* **2014** *161*, A213-A221.

[50] Leung, K., *J. Phys. Chem. C* **2013**, *117*, 1539-1547.